

# Estimating the Aerodynamic Roughness Length over Farmland Using Proba-V 300m Products

Mingzhao Yu<sup>1,2</sup>, Bingfang Wu<sup>1,\*</sup>, Qiang Xing<sup>1</sup>, Hongwei Zeng<sup>1</sup>

<sup>1</sup> Key Laboratory of Digital Earth Science, Institute of Remote Sensing and Digital Earth,

Chinese Academy of Sciences, Olympic Village Science Park, W. Beichen Road, Beijing 100101, China.

<sup>2</sup> College of Resources and Environment, University of Chinese Academy of Sciences, Beijing 100049, China.

\*Corresponding author, e-mail: wubf@radi.ac.cn

**Abstract**—The aerodynamic roughness length  $z_{0m}$  is a crucial parameter for reliably simulating the turbulent exchange between land surface and atmosphere. In this study, based on the normalized difference vegetation index (NDVI), a new vegetation index—the hotspot-darkspot vegetation index (HDVI)—is proposed to improve the quantitative estimation of the aerodynamic roughness length over farmland. To obtain this new index, the normalized-difference hotspot-darkspot index (NDHD) is introduced using a semi-empirical, kernel-driven, bidirectional reflectance model with multi-temporal Proba-V 300-m top-of-canopy (TOC) reflectance products. The linear relationship between HDVI and  $z_{0m}$  can be determined in the crop growth period. Results show that the relationship between HDVI and  $z_{0m}$  is more pronounced than that between NDVI and  $z_{0m}$ . These differences probably originate from the crop-ripening stage and harvest period, indicating that the significant impact of the crop residue on  $z_{0m}$  can be captured by NDHD. In addition, the estimated aerodynamic roughness is utilized to calculate evapotranspiration (ET) in the ETWatch system to evaluate the ET improvement with Eddy Correlation(EC) measured latent heat flux, which shows that the new estimated method for  $z_{0m}$  can improve the accuracy of ET calculation over farmland effectively.

**Keywords**—aerodynamic roughness, HDVI, NDVI, Proba-V, ET

## I. INTRODUCTION

The aerodynamic roughness length  $z_{0m}$  is the height above the ground where the wind speed is zero under neutral conditions. It plays an important role in land surface fluxes simulation and atmospheric boundary studies.

The traditional method for calculating  $z_{0m}$  is based on measurements of wind profiles over the ground under neutral atmospheric conditions, while it is unrealistic to measure wind profiles over all the surfaces in a large scale. Many researchers simply got  $z_{0m}$  values from a look-up table, which is closely related to the local topography and land use types. While these look-up approaches ignore the inherent temporal and spatial variability of land cover. For farmland in particular, crops grow rapidly in growing season and the diverse canopy characteristics lead to difference in  $z_{0m}$ . In early studies,  $z_{0m}$

was usually described as simple fractions of the vegetation height. Typically,  $z_{0m}$  is roughly equal to 0.13h. However, it is obvious that vegetation height is not the only factor in determining traits, the canopy structure and the plant density still play important roles in aerodynamic roughness over farmland.

Recently, remote sensing has been an effective way to retrieve surface information and parameterize aerodynamic roughness spatially, and several models have been developed for  $z_{0m}$  as functions of vegetation indexes from remote sensing data, nevertheless, the capacity of vegetation index is limited to retrieve the three-dimensional vegetation structures which closely related to  $z_{0m}$ .

Multi-angular observation can capture the uneven scattering of sunlight by vegetation. It has been reported that the Hotspot-Dark-spot index (HDS), calculated from multi-angular optical remote-sensing data, and adequately represented the geometric structures of vegetation. The objective of this study is bringing in multi-angular optical remote sensing info into  $z_{0m}$  calculation.

The new launched PROBA-V satellite offers daily reflectance in the visible and near infrared range. The optical design of PROBA-V consists of three cameras, providing wide view angles of  $\pm 51^\circ$  from nadir which include abundant directional effects in the surface reflectance. Thus the BRDF of each pixel could be derived within a few days of observations. Accordingly, this paper aims to develop a new vegetation index based on BRDF parameter to describe  $z_{0m}$  over farmland. Finally, the calibration and validity of the new index is tested using field-based measurements of wind profiles data.

## II. MATERIAL AND METHODS

### A. Study area

The study area is located in the middle reach of the Heihe River Basin (98°57'–100°52'E, 38°39'–39°59'N) in Gansu Province, which is the main irrigation agriculture economic zone and main water consumption area in the Heihe River Basin (Figure 1). The Yingke AWS is located in a typical oasis in the middle reach of the Heihe River Basin on very flat terrain and is surrounded by the Gobi Desert. The observational equipment includes a 40-m high tower with the instruments facing north to measure the wind speed, wind

direction, atmosphere temperature and humidity at different heights. The main crop near the site is irrigated spring maize.

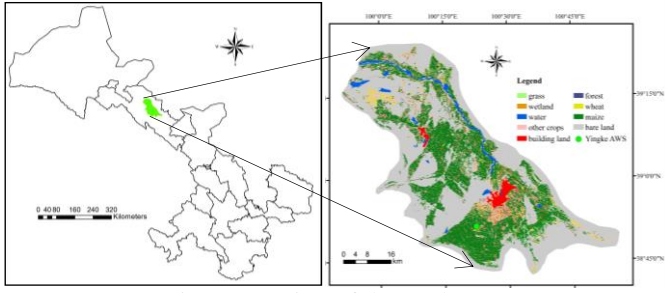


Fig.1. Location of the study area

### B. In Site Date

The AWS system at Yingke site collected data on wind speed, wind direction, air temperature and air humidity at 10-min intervals (Table 1). To guarantee the reliability of the wind profile results, the raw datasets were selected to obtain highly accurate aerodynamic roughness values based on the following criteria: (1) the wind speed is greater than 1 m/s; (2) the wind friction velocity  $u_*$  exceeds 0.2 m/s; and (3) data obtained on rainy days are discarded. Two years' data at maize growing period were processed respectively, site data of 2014 was used for model calibration and data of 2015 was for validation.

**Table 1.** Details about the Yingke AWS observation site

Coordinates	Land Use	Sensor		Period
		Height (m)		
38°51'20"N, 100°22'20"E	Spring maize	3, 5, 10, 15,	20140519-20141026	
		20, 30, 40	20150503-20151028	

### C. Satellite data

The Proba-V 300 m TOC products were acquired for 2014 and 2015 in the middle reach of the Heihe River Basin based on the spring maize phenology in Yingke. Two images (Titles: X27Y03 and X28Y03) were needed to cover the middle reach of the Heihe River Basin. The required data groups including the solar zenith angles (SZA), solar azimuth angles (SAA), viewing zenith angles of the visible and NIR (VNIR) detector (VZA), viewing azimuth angles of the VNIR detector (VAA), quality control, and the TOC reflectances of RED and NIR were extracted and converted to image files from the original HDF5 files. The images were mosaicked and clipped to the study area, projected to Albers conical equal area projections, and resampled using the bilinear interpolation method.

### D. Ground $z_{0m}$ calculation

Aerodynamic surface roughness length can be iterated out according to the wind profile data. From Monin-Obukhov similarity, roughness length and zero-plane displacement are related under neutral conditions via the logarithmic wind profile equation:

$$u = \frac{u_*}{k} \left[ \ln \left( \frac{z-d}{z_{0m}} \right) - \Psi_m \left( \frac{z-d}{L} \right) \right] \quad (1)$$

$$\theta = \frac{\theta_*}{k} \left[ \ln \left( \frac{z-d}{z_{0h}} \right) - \Psi_h \left( \frac{z-d}{L} \right) \right] + \theta_0 \quad (2)$$

where  $u$  and  $\theta$  is the wind speed and potential air temperature at height  $z$  above ground level,  $u_*$  is the friction velocity,  $\theta_*$  is friction temperature,  $k$  is von Karman's constant ( $k=0.4$ ),  $d$  is the zero-plane displacement,  $z_{0m}$  is the surface roughness length,  $z_{0h}$  is the thermal roughness length,  $L$  is the function of friction velocity, friction temperature and temperature, called the Monin-Obukhov length,  $\Psi_m$  and  $\Psi_h$  is the stability functions. The expressions of the stability functions  $\Psi_m$  and  $\Psi_h$  depend on the stability conditions in the surface layer, described by the stability parameter  $Z/L$ .

### E. NDHD calculation with Ross-Li model

The Semi-empirical kernel driven BRDF models is generally used in correcting BRDF effects and retrieving of surface albedo from multi-angle datasets, which relies on the weighted sum of an isotropic parameter and two kernels of viewing and illumination geometry to determine reflectance. The Ross-Li-Maignan model as:

$$R(\theta_i, \theta_r, \varphi) = f_{iso}(\lambda) + f_{vol}(\lambda)K_{vol}(\theta_i, \theta_r, \varphi) + f_{geo}(\lambda)K_{geo}(\theta_i, \theta_r, \varphi) \quad (3)$$

In Equation (3), surface reflectance ( $R$ ) is expressed as a combination of the function of three components. The relative azimuth  $\varphi = \varphi_i - \varphi_r$ .  $f_{iso}$  is the reflectance acquired by nadir observation when the solar zenith angle is zero.  $K_{vol}$  describes the volume scattering kernel caused by a horizontal layer of randomly distribution leaves and  $K_{geo}$  describes the surface scattering kernel caused by shadows of natural objects. They are only the functions of solar and sensor geometry, including the solar zenith ( $\theta_i$ ), view zenith ( $\theta_r$ ) and relative azimuth angles ( $\varphi$ ).  $f_{vol}(\lambda)$  and  $f_{geo}(\lambda)$  are the spectrally dependent BRDF kernel coefficients.

To calculate the kernel coefficients, we applied a multiple linear regression fit with 21-day series of reflectance and angles data. As the model is relatively insensitive to noisy data, here we use PROBA-V's quality control file to judge each pixel's quality flag, getting rid of the cloudy and invalid pixels. For a specific pixel, if at least five cloud-free observations of the surface are available during a 21-day period, kernel coefficients are calculated, otherwise invalid value assigned to it. According to the kernel coefficients, the reflectances of NIR band can be simulated from the back-scattering region to the forward-scattering region, then the Normalized Difference Hotspot Darkspot index (NDHD) was described as the normalized difference between the hot spot reflectance ( $\rho_{HS}$ ) and the dark spot reflectance ( $\rho_{DS}$ ):

$$NDHD = \frac{\rho_{HS} - \rho_{DS}}{\rho_{HS} + \rho_{DS}} \quad (4)$$

### F. Proposal of HDVI

In this study daily NDVI images are generated from PROBA-V's RED band and NIR band. Based on the quality control file, time series of 5-day composite NDVI at 300m resolution are acquired to rule out the disturbance of cloudy pixels. Considering that both NDVI and NDHD have positive correlation with  $z_{0m}$  but in different aspects, we propose a new vegetation index called the Hotspot-darkspot Vegetation Index (HDVI) defined by Equation (5):

$$HDVI = NDVI \times (1 + NDHD) \quad (5)$$

Compared with NDVI, HDVI has wider range and possibility to exceed 1. It is expected that the exponential algorithm in describing  $z_{0m}$  can be replaced after introduction of NDHD, so we try to use a linear relationship between HDVI and  $z_{0m}$  to map  $z_{0m}$  as follows:

$$z_{0m} = a \times HDVI + b \quad (6)$$

## III. RESULTS AND DISCUSSION

### A. Relationship between NDVI/HDVI and $z_{0m}$

For Yingke site, the temporal variations of the aerodynamic roughness, as deduced from the values of each five-day, reflects the process of crop growth, with a characteristic rise and fall which depicts a crop growth cycle. Fig. 2 reported the field observed aerodynamic roughness ( $z_{0m}$ ) respectively have been plotted as a linear function of NDVI and HDVI in Yingke Site. This clearly proved that NDVI of cropland has correlation with  $z_{0m}$  ( $R^2 = 0.636$ ,  $n = 33$ ), while the data are less dispersed and the correlation is higher ( $R^2 = 0.793$ ,  $n = 33$ ) when  $z_{0m}$  is plotted as a function of HDVI (Fig.2b). The results show that all optimal regression equations pass significance testing of 0.05, which meet the statistical demand ( $p < 0.05$ ). The RMSE values between the two datasets are 0.042 and 0.034, respectively, which are lower than 0.1, indicating consistency between  $z_{0m}$  and vegetation indexes.

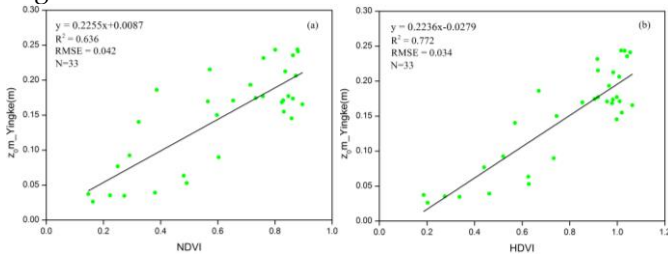


Fig.2 Observed aerodynamic roughness as a function of (a) NDVI (b) HDVI. The data was selected during the growth period of spring maize from April to October 2014 at Yingke Site.

Coefficients a and b of Equation (6) are acquired for spring maize from the linear fitting results at the Yingke. The

results are shown in Table 2. Results of the F-test suggest that the fitted models with  $p$ -values lower than 0.01, indicating a significant relationship between HDVI/NDVI data and field observed  $z_{0m}$  at the 99% confidence level.

**Table 2.** Statistical results of 2014 at Yingke Site

Location	Yingke	
Crop Type	Spring Maize	
Number of points	33	
Correlation with $z_{0m}$	HDVI	NDVI
a	0.2236	0.2255
b	-0.0279	0.0087
$R^2$	0.772	0.636
RMSE	0.034	0.042
MAE	0.027	0.031
Durbin-Watson statistic	1.338	0.927
F-statistics	15.435	12.734
$p$ -value	$4.39 \times 10^{-12}$	$6.48 \times 10^{-11}$

### B. Regional-Scale $z_{0m}$

To compare the difference in spatial distribution between NDVI and HDVI, we select two days' data (August 12th represents the peak growth stage and October 1st represents the mature period of spring maize, respectively) to make the NDVI and HDVI map, shown in fig.3. Because of the introduction of BRDF signatures, HDVI showed spatial distribution discrepancy compared with NDVI, especially on October 1st.

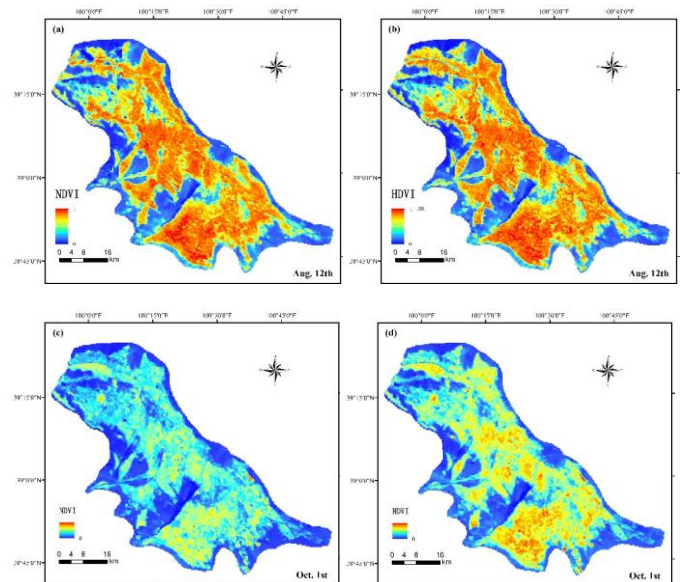


Fig.3 Map of (a) NDVI on Aug. 12th, (b) HDVI on Aug. 12th, (c) NDVI on Oct. 1st, (d) HDVI on Oct. 1st in the middle reach of the Heihe River Basin.

### C. Validation of the $z_{0m}$ results

The aerodynamic roughness length of 2015 at Yingke Site was calculated using the same coefficients as 2014. The AWS data of 2015 was used to validate the remote sensing model. Results of 2015 showed high correlation between the observed  $z_{0m}$  and estimated  $z_{0m}$ , with a coefficient of determination of 0.787(Fig.4), which proved that the method can be broadened to any growth period for a certain crop.

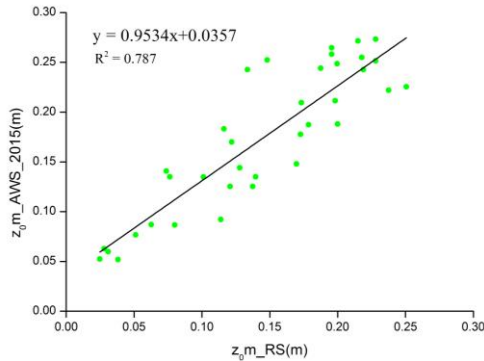


Fig.4 Comparison between the estimated aerodynamic roughness length from remote sensing data and the observed  $z_{0m}$  from Yingke's AWS data of 2015.

### D. Application of $z_{0m}$ in ET estimation model

According to the estimated  $z_{0m}$  results of Yingke Site, we collected some metrological data from ground meteorological stations in the middle reach of Heihe River Basin in 2014 to test  $z_{0m}$  in actual evapotranspiration calculation. The observed ET was measured by the eddy covariance (EC) data at Yingke site. ETWatch model was used to test the improvement of aerodynamic roughness model here, Other input parameters were kept the same but two different  $z_{0m}$  datasets were prepared, respectively. For the results of Fig. 5(a), the  $z_{0m}$  was calculated from the empirical relationship with the vegetation height data which observed at Yingke Site, the estimated  $z_{0m}$  value was input and calculating new ET results which showed in Fig. 5(b). According to the comparison results of correlation analysis showed in Figure 5, the results from the improved  $z_{0m}$  model shows slightly better overall agreement with the ET measured by EC.

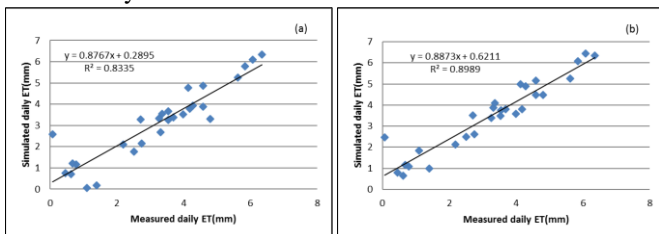


Fig.5 Comparison of the daily ET derived from (a) input fixed values of  $z_{0m}$ , (b) input the improved  $z_{0m}$  value from our model with EC tower-based measurements.

## IV. CONCLUSION

Satellite-based algorithms are now routinely applied to retrieve terrestrial parameter such as aerodynamic roughness with the development of remote sensing technology. This paper made an improved model for estimating  $z_{0m}$  over cropland. The introduction of BRDF signatures makes the model more accurate and persuasive, for the reason that the multi-angle remote sensing data has irreplaceable advantages in describing crop canopy structure. As crops growing on farmland are characterized by uniformly distributed and flat, by contrast, we can neglect the topography change and break up aerodynamic roughness into two parts: vertical roughness associated with crop growth condition and horizontal roughness associated with crop planting structures. In our model, NDVI still plays the leading role to reflect crop growth condition, using NDHD to express the variations of vegetation spatial structure as assistance, satisfactory results of aerodynamic roughness length estimation are obtained. The method move away from dependence on vegetation height and develop a pure remote sensing model, improving the timeliness put forward for aerodynamic roughness estimation.

## V. ACKNOWLEDGMENT

This work was supported in part by Advanced Science Foundation Research Project of the Chinese Academy of Sciences (Grant No.: QYZDY-SSW-DQC014) and the Natural Science Foundation of China, Grant No. 41271424. We thank VITO for providing the Proba-V 300 m products. The authors also thank the Environmental and Ecological Science Data Center for West China, National Natural Science Foundation of China for providing the AWS data and land cover map (<http://westdc.westgis.ac.cn>).

## VI. REFERENCES

- [1] Liou Y.A., Galantowicz J.F, England A.W. "A land surface process/radio brightness model with coupled heat and moisture transport for prairie grassland." J. IEEE Trans. Geosci. Remote Sens. 1999, 37, 1848-1859.
- [2] Hryama, T., Sugita, M., Kotoda, K. "Regional roughness parameters and momentum fluxes over a complex area." J. Appl. Meteorol. 1996, 35, 2179-2190.
- [3] Borak, J.S., Jasinski, M.F., Crago, R.D. "Time series vegetation aerodynamic roughness fields estimated from MODIS observations." Agric. For. Meteorol. 2005, 135, 252-268.
- [4] Gupta, R.K., Prasad, T.S., Vijayan, D. "Estimation of roughness length and sensible heat flux from WiFS and NOAA AVHRR data." Adv. Space Res. 2002, 29, 33-38.
- [5] Gao, F., Schaaf, C.B., Strahler, A.H. "Detecting vegetation structure using a kernel-based BRDF model." Remote Sens. Environ. 2003, 86, 198-205.
- [6] Wanner, W., Li, X., Strahler, A.H. "On the derivation of kernels for kernel - driven models of bidirectional reflectance." J. Geophys. Res. Atmos. 1995, 100, 21077-21089.
- [7] Lacaze, R., Chen, J.M., Roujean, J.L. "Retrieval of vegetation clumping index using hot spot signatures measured by POLDER instrument. Remote Sens." Environ. 2002, 79, 84-95.
- [8] Zhong, B., Ma, P., Nie, A., Yang, A., Yao, Y., Lü, W., Zhang, H., Liu, Q. "Land cover mapping using time series HJ-1/CCD data." Sci. China Earth Sci. 2014, 57, 1790-1799.